Sea ice contribution to the air–sea CO_2 exchange in the Arctic and Southern Oceans

By SØREN RYSGAARD[1,2]*, JØRGEN BENDTSEN[1,3], BRUNO DELILLE[4], GERHARD S. DIECKMANN[5], RONNIE N. GLUD[1,6], HILARY KENNEDY[7], JOHN MORTENSEN[1], STATHYS PAPADIMITRIOU[7], DAVID N. THOMAS[7,8] and JEAN-LOUIS TISON[9], [1]*Greenland Climate Research Centre, Greenland Institute of Natural Resources, Kivioq 2, 3900 Nuuk, Greenland;* [2]*Centre for Earth Observation Science, CHR Faculty of Environment Earth and Resources, University of Manitoba, 499 Wallace Building, Winnipeg, MB R3T 2N2, Canada;* [3]*Centre for Ice and Climate, Niels Bohr Institute, University of Copenhagen, Juliane Maries vej 30, 2100 Copenhagen O, Denmark;* [4]*Unité d'Oceanographie Chimique, Interfacultary Centre for Marine Research, Université de Liége, Allée du 6 Août, 17, 4000 Liège, Belgium;* [5]*Alfred Wegener Institute for Polar and Marine Research, Am Handelshafen 12, 27570 Bremerhaven, Germany;* [6]*Scottish Association of Marine Sciences, Scotland UK, Southern Danish University and NordCee, Odense M, Denmark;* [7]*School of Ocean Sciences, Bangor University, Menai Bridge, Anglesey LL59 5AB, Wales, United Kingdom;* [8]*Finnish Environment Institute (SYKE), Marine Research Centre, Erik Palmenin aukio 1, P.O. Box 140, FI – 00251 Helsinki, Finland;* [9]*Glaciology Unit, Department of Earth and Environmental Sciences, Université Libre de Bruxelles, CP 160/03, 50 Ave. F. D. Roosevelt, 1050 Bruxelles, Belgium*

ABSTRACT

Although salt rejection from sea ice is a key process in deep-water formation in ice-covered seas, the concurrent rejection of CO_2 and the subsequent effect on air–sea CO_2 exchange have received little attention. We review the mechanisms by which sea ice directly and indirectly controls the air–sea CO_2 exchange and use recent measurements of inorganic carbon compounds in bulk sea ice to estimate that oceanic CO_2 uptake during the seasonal cycle of sea-ice growth and decay in ice-covered oceanic regions equals almost half of the net atmospheric CO_2 uptake in ice-free polar seas. This sea-ice driven CO_2 uptake has not been considered so far in estimates of global oceanic CO_2 uptake. Net CO_2 uptake in sea-ice–covered oceans can be driven by; (1) rejection during sea–ice formation and sinking of CO_2-rich brine into intermediate and abyssal oceanic water masses, (2) blocking of air–sea CO_2 exchange during winter, and (3) release of CO_2-depleted melt water with excess total alkalinity during sea-ice decay and (4) biological CO_2 drawdown during primary production in sea ice and surface oceanic waters.

1. Introduction

Understanding the CO_2 exchange between atmosphere, ocean and land is crucial since global marine and terrestrial systems currently absorb about half of the CO_2 emitted by fossil-fuel combustion (Sabine et al., 2004). Although the geographical and seasonal data coverage of CO_2 exchange rates is increasing, large gaps still exist in remote areas, particularly over the oceans (Takahashi et al., 2009). The role of ice-covered oceans in the CO_2 balance has been largely ignored because continuous

sea-ice cover is assumed to impede gaseous exchange with the atmosphere so efficiently that no global models include CO_2 exchange over sea ice (Tison et al., 2002). Although salt rejection from sea ice has been recognized as an important process leading to deep-water formation and thereby strengthening the deep thermohaline circulation in the world ocean, the implications of the concurrent rejection of total dissolved inorganic carbon ($[TCO_2] = [CO_2] + [HCO_3^-] + [CO_3^{2-}]$) for the air–sea CO_2 flux have received little attention. Currently, the TCO_2 and CO_2 flux mechanisms associated with sea ice in polar seas are driven by the aforementioned sea ice–ocean TCO_2 transport (Anderson et al., 2004; Rysgaard et al., 2007; Semiletov et al., 2004) and air–sea CO_2 exchange mediated by biological, physical and chemical changes in sea-ice brines (Jones and Coote,

*Corresponding author.
e-mail: rysgaard@natur.gl

1981; Gleitz et al., 1995; Tison et al., 2002; Delille et al., 2007; Dieckmann et al., 2008, 2010; Jones et al., 2010) and in surface oceanic waters (Rysgaard et al., 2009; Jones et al., 2010). Here, we report a conceptual model on the season-dependent processes by which sea ice controls air–sea CO_2 exchange, and quantify the air–sea flux of CO_2 modulated by sea ice formation and decay.

2. Results and discussion

2.1. Conceptual model of seasonal carbon fluxes in ice-covered seas

The processes driving air–sea gas exchange are active throughout the cycle of sea-ice formation and decay (Fig. 1). The manner in which these processes impact on gas exchange is largely dependent on the physical controls on ice structure, such as changes in porosity, ultimately a function of bulk sea-ice temperature and salinity (S) (Cox and Weeks, 1983). As air and surface oceanic temperatures decrease in autumn, sea ice begins to form as a porous ice crystal matrix filled with a hypersaline solution (sea ice brine; $S_{brine} > 35$) resulting from the rejection of dissolved salts from the ice matrix. As a result of the physical

concentration of dissolved salts during sea ice formation, concentrations of TCO_2 and CO_2 as well as other gases in the brine are high (Glud et al., 2002). At this early stage, the sea ice is still permeable to liquid and gas exchange because of elevated porosity (Weeks and Ackley, 1986; Golden et al., 1998, 2007; Petrich and Eicken, 2010). As a consequence, and due to the ice and brine volume contracting on rapid surface cooling, a small fraction of the CO_2-supersaturated brine is transported upwards through the sea-ice column and expelled onto the ice surface, resulting in a CO_2 efflux to the atmosphere (Nomura et al., 2006; Delille et al., 2007). However, by far the largest flux of TCO_2 and CO_2 is driven by brine drainage to the under-ice water and subsequent incorporation into intermediate and deep-water masses (Rysgaard et al., 2007; Sejr et al., 2011). As a result of this process, CO_2 supersaturation has been observed below sea ice in the Arctic Ocean (Kelley, 1967; Semiletov et al., 2004), and in coastal Antarctic areas (Gibson and Trull, 1999), while high TCO_2 concentrations have been measured below Arctic sea ice during winter (Anderson et al., 2004; Rysgaard et al., 2007). Concurrent rejection of TCO_2 and CO_2 has also been documented in experimental ice tank studies (Killawee et al., 1998; Papadimitriou et al., 2003; Rysgaard et al., 2007). Significant brine transport below the surface layer and contribution
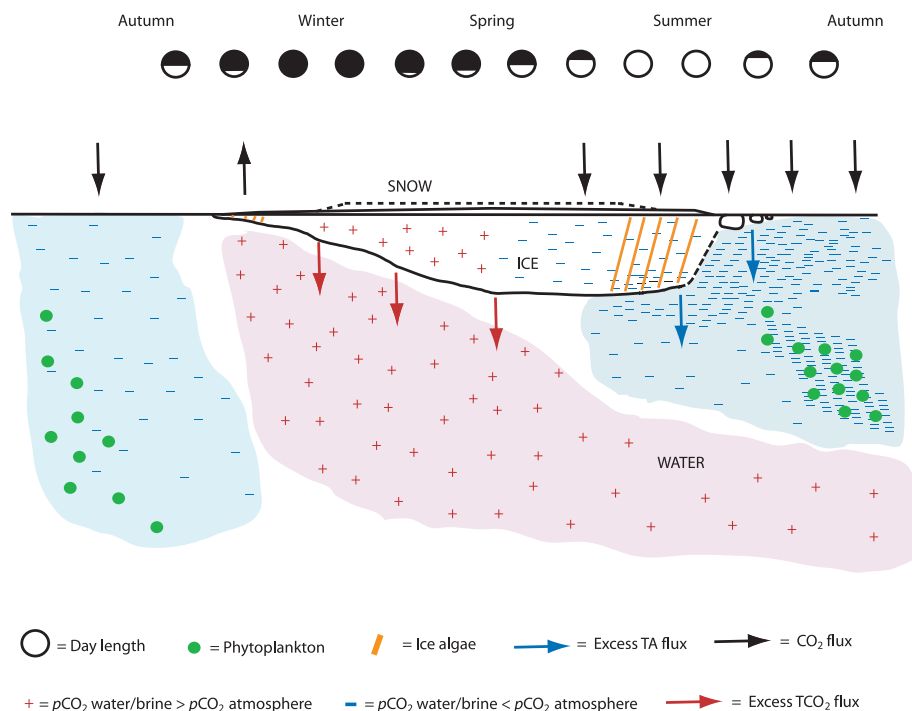

Fig. 1. Conceptual model of seasonal carbon fluxes in ice-covered seas. The figure covers the upper 100 m of the water column. The processes driving air–sea gas exchange are active throughout the cycle of sea ice formation and decay. During winter, ice growth results in the rejection of CO_2 along with salts dissolved in seawater from the ice crystal matrix, which gives rise to dense brine that sinks and is incorporated into intermediate and deep water layers. Subsequent sea ice melt during the summer thaw results in the formation of a strong halocline, with surface waters well below atmospheric CO_2 saturation, thus enhancing the uptake of atmospheric CO_2 from the ocean. In addition, primary productivity in both sea ice and water column helps reduce surface-water CO_2 concentrations further, enhancing the air–sea CO_2 flux.

to deep-water formation has been observed in coastal polynyas, where sea ice is formed continuously via increases in bottom-water salinity (Shcherbina et al., 2003; Skogseth et al., 2004), and via tracer studies on Arctic shelves (Bönisch and Schlosser, 1995). Dense intermediate water masses formed by brine release from sea ice have been observed in the Okhotsk Sea (Shcherbina et al., 2003), in Storfjorden on Svalbard (Rudels et al., 2005), and on the shelves of the Canada Basin (Yamamoto-Kawai et al., 2009). The above clearly indicates that sea ice formation must drive a flux of TCO$_2$ and CO$_2$ to the underlying seawater along with brine generated in the process. Subsequent removal of this amount of TCO$_2$ from the surface oceanic mixed layer to deeper water masses via sinking of the expelled dense brine, in conjunction with dilution by a mixture of meltwater when sea ice melts later in the year, will both lead to a reduction of surface-water CO$_2$(aq) (aqueous form of CO$_2$) and a subsequent increase in the air–sea CO$_2$ flux.

During winter, as sea ice continues to grow, reduced air temperatures cause the brine volumes of surface sea ice to contract and permeability to decrease, effectively stopping air–sea ice gas exchange (Rysgaard et al., 2007; Loose et al., 2011). Brine volume contraction during winter further increases brine salinity, CO$_2$(aq) and supersaturation with respect to a suite of minerals, including several polymorphs of calcium carbonate (CaCO$_3$) (Assur, 1960), such as ikaite (Dieckmann et al., 2008, 2010). Precipitation of CaCO$_3$ [Ca^{2+} + 2HCO$_3^-$ → CaCO$_3$(s) + H$_2$O + CO$_2$(aq)] from the brine lowers total alkalinity (TA) and further increases the concentration of CO$_2$(aq) in the brine. The specific conditions promoting CaCO$_3$ precipitation in sea ice are currently poorly understood, but if precipitation occurs in the porous bottom sea-ice layer, where the brine volume is less than 5% (Weeks and Ackley, 1986; Golden et al., 1998, 2007), the CO$_2$-enriched brine will exchange with seawater via gravity drainage (Notz and Worster, 2009). In contrast, the CaCO$_3$ crystals will potentially remain trapped within the skeletal layer, where they will act as a store of TA, which will become a source of excess TA to the oceanic water upon subsequent mineral dissolution (Rysgaard et al., 2007, 2009; Nedashkovsky et al., 2009). Other potential winter air–sea gas exchange pathways are via sea-ice flooding events (Antarctica) and gas diffusion from the ice matrix and from openings in the ice structure.

As temperatures rise during spring and summer, the sea ice melts, resulting in a brine volume expansion and an increase in sea-ice permeability (Cox and Weeks, 1983; Golden et al., 1998). Increasing porosity enhances the potential for CO$_2$ exchange between air, sea ice and the underlying oceanic water. Brine initially supersaturated with CO$_2$ will become a source of CO$_2$ to the atmosphere. However, rapid brine dilution through internal ice melt will lead to a reduction in the CO$_2$(aq) concentration, which can be further enhanced by the increase in TA associated with CaCO$_3$ dissolution. Such conditions may eventually favour reversion of the CO$_2$ flux, turning sea ice into a CO$_2$ sink. Photosynthetic activity by ice algae causes a further, and

often extensive, reduction in brine concentrations of TCO$_2$ and CO$_2$(aq) (Gleitz et al., 1995) when light availability increases due to insulation and gradual snow melt (Horner and Schrader, 1982).

Sea-ice melt leads to stratification of the surface water column and mixing with melt water already low in TCO$_2$ from biological uptake and excess TA from the internal sea-ice CaCO$_3$ cycle. The net result will be an increase in TA and a lowering of CO$_2$(aq) in the stratified surface waters, enhancing the air–sea CO$_2$ flux (Rysgaard et al., 2007, 2009). Evidence of excess TA via sea-ice–derived CaCO$_3$ dissolution has been observed in the top few hundred metres in Baffin Bay following ice melt (Jones et al., 1983), in the upper layers of the Arctic Ocean (Rysgaard et al., 2009), and in coastal areas of East Greenland (Sejr et al., 2011). Sea ice break-up also enhances light availability in surface waters, which triggers pelagic primary production (Horner and Schrader, 1982; Mikkelsen et al., 2008), thereby further reducing surface-water CO$_2$(aq). Primary production continues throughout the summer, and algal cells sinking from the euphotic zone result in a net export of carbon (biological pump) (Rysgaard et al., 1998, 1999).

At present, it is difficult to distinguish between the respective roles of sea-ice–driven and pelagic productivity-driven air–sea CO$_2$ exchange on a large scale, but the pelagic biological pump and the sea ice pump have recently been estimated to be of equal size in the northeastern Greenland Sea (Rysgaard et al., 2009).

2.2. Quantification of the sea ice–water flux of CO$_2$ in ice-covered seas

By applying our conceptual model outlined above and shown schematically in Fig. 1, the air–sea CO$_2$ flux can be determined from recent estimates of seasonal changes in sea ice volume and measured TCO$_2$ and TA concentrations (Table 1). The volume of Arctic sea ice can be estimated at 8480 km^3 based on the seasonal ice cover (Comisio and Nishio, 2008) and an average thickness of 1.06 m (Kwok et al., 2009). Similarly, the sea-ice volume in the Antarctic is estimated at 9920 km^3 based on seasonal cover (Comisio, 2010) and an average thickness of 0.62 m (Worby et al., 2008). The bulk salinity and TCO$_2$ and TA concentrations (per kilogram of melted sea ice) representative of Arctic sea ice are estimated at 4.0, 300 μmol kg^{-1}, and 540 μmol kg^{-1}, respectively (Rysgaard et al., 2009), while the equivalent estimates representative of Antarctic sea ice are, 6.0, 480 μmol kg^{-1} and 864 μmol kg^{-1}, respectively, based on the relationship of TCO$_2$ and TA to bulk sea-ice salinity in the Arctic (above refs) and the bulk salinity distribution in Antarctic sea ice (Rysgaard et al., 2009; Jones et al., 2010). To our knowledge, no direct measurements of TCO$_2$ and TA have been reported from Antarctic sea ice. Representative water-column conditions of salinity, TCO$_2$ and TA in the upper 50 m in the Arctic Ocean are 31.70, 1810 μmol kg^{-1} and 1928 μmol kg^{-1}, respectively (Rysgaard et al., 2009), while the equivalent surface

Table 1. Quantification of CO_2 fluxes in ice-covered seas

	Arctic	Antarctic	Total
Volume of seasonal ice[a]	8480 km^3	9920 km^3	18 400 km^3
Sea ice parameters[b]	Salinity = 4	Salinity = 6	
	$TCO_2 = 300\ \mu$mol kg^{-1}	$TCO_2 = 480\ \mu$mol kg^{-1}	
	TA = 540 μmol kg^{-1}	TA = 864 μmol kg^{-1}	
Water-column parameters[c]	Salinity = 31.70	Salinity = 33.98	
	$TCO_2 = 1810\ \mu$mol kg^{-1}	$TCO_2 = 2219\ \mu$mol kg^{-1}	
	TA = 1928 μmol kg^{-1}	TA = 2361 μmol kg^{-1}	
Gross transport of TCO_2 from sea ice to water column	138 Tg C yr^{-1}	186 Tg C yr^{-1}	324 Tg C yr^{-1}
Net CO_2 air–sea flux due to sea ice melt (sea ice TA : TCO_2 = 1.06)[d]	−14 Tg C yr^{-1}	−19 Tg C yr^{-1}	−33 Tg C yr^{-1}
Net CO_2 air–sea flux due to sea ice melt (sea ice TA : TCO_2 = 1.80)[e]	−31 Tg C yr^{-1}	−52 Tg C yr^{-1}	−83 Tg C yr^{-1}
Open water polar oceans	−154 Tg C yr^{-1}	−45 Tg C yr^{-1}	−199 Tg C yr^{-1}
CO_2 air-sea flux (Takahashi et al. 2009)	(90°N to 62°N)	(50°S to 90°S)	
Sea ice CO_2 pump in% of total net uptake (Takahashi et al. 2009)			17–42%[f]

[a]Based on seasonal ice cover in the Arctic (Comisio and Nishio, 2008) with an average thickness of 1.06 m (Kwok et al., 2009) and seasonal ice cover in the Antarctic (Comisio, 2010) with an average thickness of 0.62 m (Worby et al., 2008).

[b]μmol kg^{-1} melted sea ice.

[c]Mean of 50 m mixed layer.

[d]Represents conditions without $CaCO_3$ formation in sea ice.

[e]Represents conditions with $CaCO_3$ formation in sea ice.

[f]This uptake will double if model-derived seasonal sea ice volumes are used (McLaren et al., 2006).

oceanic water conditions in the polar Southern Ocean are 33.98, 2219 μmol kg^{-1} and 2361 μmol kg^{-1}, respectively (Eicken, 1992; Jones et al., 2010). Using the above data as initial conditions of the surface oceanic water mass from which sea ice is formed upon freezing (assuming that sea ice is only formed once) an estimate of the gross TCO_2 rejection flux via brine generation and rejection from sea ice to the underlying oceanic water can be computed. In the Arctic ocean, the total TCO_2 stored in the annually produced sea ice then corresponds to 27.5 Tg C whereas the TCO_2 in the surface water from which the sea ice was formed contained 165.8 Tg C. The difference corresponds to an annual flux of 138 Tg C yr^{-1} occurring in the Arctic between surface water and sea ice. Together with the corresponding gross fluxes around Antarctica of 186 Tg C yr^{-1} this yields a global ocean-sea ice gross flux of 324 Tg C yr^{-1} (Table 1). On larger time scales, the accumulated fluxes become significant and underline the importance of sea ice formation in the oceanic carbon cycle and its potential for long-term control of atmospheric CO_2 levels.

2.3. Estimates of the air–sea flux of CO_2 in ice-covered seas

Transport of TCO_2 with rejected brine to below the surface mixed oceanic layer during sea ice formation, and subsequent melting of sea ice during the summer thaw may, in combination, result in under-saturated CO_2 conditions in surface waters relative to the atmosphere, driving a net air-sea CO_2 flux. An upper bound on the increased air–sea CO_2 flux under these conditions can be estimated by considering the mass balance in a well mixed surface layer with a constant depth. This simple mixed layer model does not explicitly account for the seasonal changes in mixed layer depth, heat content and concentrations of salinity and dissolved inorganic carbon substances. However, the model quantifies the expected perturbation of the air–sea CO_2 flux, which can be ascribed to the sea ice–ocean transport of TCO_2 and alkalinity. The amount of brine transported away from the sea ice formation region is a critical process, but we do not have enough data to constrain this export on a global scale. An upper bound on the influence on the air–sea CO_2 flux can be set by assuming that all brine is exported out of the mixed layer, and neglecting the relatively small volume of brine compared to the mixed layer volume (Rysgaard et al., 2007). Also, we assume that lowering of the surface $CO_2(aq)$ due to the sea ice melt will result in an excess atmospheric CO_2 flux until the mixed layer $CO_2(aq)$ concentration returns to its initial value. This implies that the surface layer is exposed for sufficient time (~months) such that the mixed layer can equilibrate with the atmosphere. The mixed layer is assumed to have a depth (δ_{ML}) of 50 m and we apply representative values of the initial mixed layer concentrations (φ_0) of temperature, salinity, TCO_2 and TA before sea ice is formed. Brine rejection decreases the sea ice

concentrations (φ_{ice}) of salinity, TCO$_2$ and TA, and the amount of brine transported out of the surface mixed layer therefore determines the mixed layer concentrations when sea ice melts (φ_{ML}). The mixed layer concentrations after sea ice has melted can then be determined from the maximum sea ice thickness during winter (δ_{ice})

$$\varphi_{ML} = \frac{1}{\delta_{ML}} \left[(\delta_{ML} - \delta_{ice}) \varphi_0 + \delta_{ice} \varphi_{ice} \right].$$

Due to the relatively low TCO$_2$ concentration in the sea ice, the resultant surface CO$_2$(aq) is undersaturated compared to the initial CO$_2$(aq) level before sea ice was formed. The amount of additional TCO$_2$ required to obtain the initial mixed layer CO$_2$(aq) concentration is determined, and this amount of TCO$_2$ therefore corresponds to a potential increase in air–sea CO$_2$ exchange due to the larger air–sea pCO$_2$ difference. Surface pCO$_2$ is calculated from the temperature and salinity-dependent solubility and dissociation constants of seawater (Zeebe and Wolf-Gladrow, 2001).

To determine the magnitude of this air–sea CO$_2$ flux, two calculations can be done, one assuming no CaCO$_3$ crystal formation in sea ice (TA : TCO$_2$ = 1.06 as in surface seawater), and one assuming CaCO$_3$ crystal formation in sea ice (TA : TCO$_2$ = 1.8, representing conditions of melted sea ice in the Fram Strait; Rysgaard et al., 2009). In the first scenario, melting of a total of 18 400 km^3 of sea ice in the Arctic and Antarctic will dilute surface-water CO$_2$, resulting in a downward net air–sea CO$_2$ flux of –33 Tg C yr^{-1} following equilibrium with the atmosphere (atmospheric pCO$_2$ = 387 ppm). In the second scenario, the net downward air–sea flux will increase to –83 Tg C yr^{-1} following equilibrium with the atmosphere. The highest air–sea CO$_2$ flux in both scenarios occurs around Antarctica. These fluxes are equivalent to 17–42% of the air–sea CO$_2$ flux in open oceanic water at high latitudes (>62°N and >50°S; Takahashi et al., 2009; Table 1). This estimate contrasts strongly with the perception that sea ice acts solely as a lid, sealing off air–sea gas exchange. Furthermore, our estimates of the air–sea CO$_2$ fluxes in the Arctic Ocean as a result of sea ice melt are equivalent to 11–26% of the net air–sea CO$_2$ flux presented by Arrigo et al., (2010), 22–49% of the CO$_2$ uptake capacity of the winter mixed layer in the Arctic Ocean (Jutterström and Anderson, 2010), and 32–70% of the estimated wintertime air–sea CO$_2$ flux for the central arctic polynyas and seasonally ice-covered arctic regions (Omar et al., 2005). More detailed data on other estimates of the air–sea CO$_2$ exchange in the Arctic Ocean have been compiled by Bates and Mathis (2009).

The above estimates are only based on overall changes in sea ice cover and not total sea ice production. The latter is larger than the former, because, from late autumn to early spring, sea ice is formed continuously in polynyas (Zhang, 2007) and is exported farther afield where it eventually melts. Model studies of ocean circulation below Antarctic sea ice show a large potential for continuous melting and freezing of sea ice during winter (Zhang,

2007). Model-derived quantification of annual mean changes in sea ice volume of 20 000 km^3 and 14 000 km^3 for the Arctic and Antarctic (McLaren et al., 2006), respectively, are significantly higher than estimates based on observed sea ice cover (cf. Table 1). Using these values would increase our estimates of net CO$_2$ air–sea exchange accordingly. It is noted that these modelled seasonal sea ice volumes based on sea ice production will cause the strongest air–sea CO$_2$ uptake flux to occur in the Arctic.

3. Priorities for future research

As the CO$_2$ transport mechanism outlined above is linked to the sea ice formation and decay cycle, future changes in global sea ice cover will affect the capacity of the polar seas for taking up atmospheric CO$_2$. To increase the accuracy of the estimate of the influence of sea ice on air–sea CO$_2$ exchange, more core data of parameters of the CO$_2$ system are needed from various types and concentrations of sea ice, for example, compact ice, consolidated ice and pack ice in all its different forms (close pack ice to open pack ice). The link between total sea ice production and melting (by volume) and the rejection of TCO$_2$ and the resultant air–sea CO$_2$ exchange in both polar seas merits dedicated investigation. In addition, more information is needed on the regional differences in TCO$_2$ rejection and its fate in the water column in various parts of the ocean at high latitudes in both hemispheres. Available measurements and estimated air–sea CO$_2$ fluxes suggest substantial variability in the Arctic Ocean (Fransson et al., 2009; Jutterström and Anderson, 2010; Arrigo et al., 2010; Cai et al., 2010; Mucci et al., 2010). The proportion of TCO$_2$ rejected along with brine during sea ice formation that enters the intermediate and deep water masses, as well as its trajectory and residence time there, are all key to the central concept presented here and warrant further research. A recent study with an intermediate complexity global carbon cycle model of the impact on the glacial atmospheric CO$_2$ conditions of the formation and rapid sinking of brines away from the surface of the ocean, showed that this brine mechanism could account for a significant decrease in atmospheric pCO$_2$ during glacial times and may even contribute to the glacial–interglacial change (Bouttes et al. 2010).

Ultimately, the importance of the sea ice carbon pump versus the solubility pump and biological carbon pump described here will be established only through such studies. It has been shown that reduced sea ice cover will facilitate an increase in primary production in the Arctic (Rysgaard et al. 1999; Arrigo et al., 2008). The importance of the biological carbon pump may therefore be expected to increase as sea ice cover is reduced. By contrast, it has been suggested recently that rapid CO$_2$ invasion from the atmosphere can act as a barrier to a continuous atmospheric CO$_2$ uptake by the Arctic Ocean, such that the Arctic Ocean basin will not become a large atmospheric CO$_2$ sink under ice free conditions (Cai et al., 2010). Changes in water mass

distributions in the upper Arctic Ocean may also increase sea ice melting in a future warmer climate (Martinson and Steele, 2001) and thereby increase the influence from melting sea ice on CO_2(aq) levels in the surface water.

Another unknown factor is the function of polynya areas relative to the air–sea CO_2 flux. In polynya areas there is contact between water and air but at present we know too little of the mechanisms controlling this air–sea gas exchange. The under-ice mixed waters in the seasonal ice zone in the Southern Ocean may in many places exceed atmospheric values (Takahashi et al., 2009) and could be a CO_2 source if exposed to the air. As stated above the mechanism behind this exchange is not well understood and we lack data. It may even be likely, considering the relatively long equilibration time of CO_2 in the surface layer, that a polynya acts as a downward vertical transport mechanism to remove CO_2(aq) rejected from sea ice away from the surface layer (down) by horizontal transport of CO_2(aq) rich water from ice covered regions into the polynya area. Hence, the polynia can act as an accelerator of the downward CO_2 flux. There will be a small flux into the air but much lower than the downward flux in the sea. At the same time, sea ice containing low bulk concentrations of CO_2(aq) and high alkalinity, is being produced and continuously removed from the area. When this sea ice melts during spring it will lower CO_2 concentrations in surface waters compared with the atmosphere. This will ensure a net CO_2 flux into the sea over the entire year.

Finally, given the vast area of sea ice-covered seas, their variety in terms of geography and the gaps in data sets of the parameters of the CO_2 system in these remote areas, further research on the sea ice-driven CO_2 transport is urgently needed as high latitude areas continue to warm.

4. Conclusion

A review has been presented of mechanisms by which sea ice directly and indirectly controls the air–sea CO_2 exchange. The processes driving air–sea gas exchange are active throughout the cycle of sea ice formation and decay. During winter, ice growth results in the rejection of CO_2 along with salts dissolved in seawater from the ice crystal matrix, which gives rise to dense brine that sinks and is incorporated into intermediate and deep water layers. Subsequent sea ice melt during the summer thaw results in the formation of a strong halocline, with surface waters well below atmospheric CO_2 saturation, thus enhancing the uptake of atmospheric CO_2 from the ocean. In addition, primary productivity in both sea ice and water column helps reduce surface-water CO_2 concentrations further, enhancing the air–sea CO_2 flux. We estimate that the gross TCO_2 rejection flux via brine generation and rejection from sea ice to the underlying oceanic water is 324 Tg C yr^{-1}, with 138 Tg C yr^{-1} occurring in the Arctic and 186 Tg C yr^{-1} in the Antarctic. Assuming that the rejected CO_2 from sea ice is exported below the mixed layer, an upper estimate of the air–sea CO_2 flux following melting of 18 400 km^3 of sea ice in the Arctic and Antarctic, with and without $CaCO_3$ crystal formation in sea ice, will result in an air–sea CO_2 flux of –83 Tg C yr^{-1}and –33 Tg C yr^{-1}, respectively. These fluxes are equivalent to 17–42% of the air–sea CO_2 flux in open oceanic water at high latitudes ($>62°$N and $>50°$S) and contrast strongly with the perception that sea ice acts solely as a lid, sealing off air–sea gas exchange.

5. Acknowledgments

References

Anderson, L. G., Falck, E., Jones, E. P., Jutterström, S. and Swift J. H. 2004. Enhanced uptake of atmospheric CO_2 during freezing of seawater: a field study in Storfjorden, Svalbard. *J. Geophys. Res.* **109**, C06004, doi:10.1029/2003JC002120.

Arrigo, K. R., Pabi, S., van Dijken, G. and Maslowski, W. 2010. Air-sea flux of CO_2 in the Arctic Ocean, 1998–2003. *J. Geophys. Res.* **115**, G04024, doi:10.1029/2009JG001224.

Arrigo, K. R., van Dijken, G. and Pabi, S. 2008. Impact of a shrinking Arctic ice cover on marine primary production. *Geophys. Res. Lett.*, **35**, L19603, doi:10.1029/2008GL035028.

Assur, A. 1960. Composition of sea ice and its tensile strength. *SIPRE Research Report* 44.

Bates, N. R. and Mathis, J. T. 2009. The Arctic Ocean marine carbon cycle: evaluation of the air-sea CO_2 exchanges, ocean acidification impacts and potential feedbacks. *Biogeosciences* **6**, 2433–2459.

Bouttes, N., Paillard, D. and Roche, D. M. 2010. Impact of brine-induced stratification on the glacial carbon cycle. *Clim. Past* **6**, 575–589.

Bönisch, G. and Schlosser, P. 1995. Deep water formation and exchange rates in the Greenland/Norwegian seas and the Eurasian Basin of the Arctic Ocean derived from tracer balances. *Prog. Oceanogr.* **35**, 29–52.

Cai, W.-J., Chen, L., Chen, B., Gao, Z., Lee, S. H. and co-authors. 2010. Decrease in the CO_2 uptake capacity in an ice-free Arctic Ocean basin. *Science* **329**, 556–559.

Comisio, J. C. 2010. Variability and trends of the global sea ice cover. In: *Sea Ice*. 2nd Edition. (eds Thomas, D. N. and Dieckmann, G. S.). Wiley-Blackwell, Oxford, UK, 205–246.

Comisio, J. C. and Nishio, F. 2008. Trends in the sea ice cover using enhanced and compatible AMSR-E, SSM/I, and SMMR data. *J. Geophys. Res.* **113**, C02S07, doi:10.1029/2007JC004257.

Cox, G. F. N. and Weeks, W. F. 1983. Equations for determining the gas and brine volumes in sea-ice samples. *J. Glaciol.*, **29**, 306–316.

Delille, B., Jourdain, B., Borges, A. V., Tison, J.-P. and Delille, D. 2007. Biogas (CO_2, O_2, dimethylsulfide) dynamics in spring Antarctic fast ice. *Limnol. Oceanogr.* **52**, 1367–1379, doi:10.4319/lo.2007.52.4.1367.

Dieckmann, G. S., Nehrke, G., Papadimitriou, S., Göttlicher, J., Steininger, R. and co-authors. 2008. Calcium carbonate as ikaite crystals in Antarctic sea ice. *Geophys. Res. Lett.* **35**, L08501, doi:10.1029/2008GL033540.

Dieckmann, G. S., Nehrke, G., Uhlig, C., Göttlicher, J., Gerland, S. and co-authors. 2010. Brief communication: ikaite (CaCO$_3$ * 6H$_2$O) discovered in Arctic sea ice. *Cryosphere Discuss.* **4**, 153–161.

Eicken, H. 1992. Salinity profiles of Antarctic sea ice: Field data and model results. *J. Geophys. Res.* **97**(C10), 15 545–15 557, doi:10.1029/92JC01588.

Fransson, A., Chierici, M. and Nojiri, Y. 2009. New insights into the spatial variability of the surface water carbon dioxide in varying sea ice concentrations in the Arctic Ocean. *Continental Shelf Res.* **29**, 1317–1328.

Gibson, J. A. E. and Trull, T. W. 1999. Annual cycle of fCO$_2$ under sea-ice and in open water in Prydz Bay, East Antarctica. *Mar. Chem.* **66**, 187–200. American Geophysical Union, Washington, DC

Gleitz, M., v.d. Loeff, M. R., Thomas, D. N., Dieckmann, G. S. and Millero, F. J. 1995. Comparison of summer and winter inorganic carbon, oxygen and nutrient concentrations in Antarctic sea ice brine. *Mar. Chem.* **51**, 81–91.

Glud, R. N., Rysgaard, S. and Kühl, M. 2002. A laboratory study on O$_2$ dynamics and photosynthesis in ice algal communities: quantification by microsensors, O$_2$ exchange rates, ^{14}C incubations and PAM fluorometer. *Aquat. Microb. Ecol.* **27**, 301–311.

Golden, K. M., Ackley, S. F. and Lytle, V. I. 1998. The percolation phase transition in sea ice. *Science* **282**, 2238–2241.

Golden, K. M., Eicken, H., Heaton, A. L., Miner, J., Pringle, D. J., and co- authors. 2007. Thermal evolution of permeability and microstructure in sea ice. *Geophys. Res. Lett.* **34**, L16501, doi:10.1029/2007GL030447.

Horner, R. and Schrader, G. C. 1982. Relative contributions of ice algae, phytoplankton and benthic microalgae to primary production in nearshore regions of the Beaufort Sea. *Arctic*, 35, 485–503.

Jones, E. P., Coote, A. R. and Levy, E. M. 1983. Effect of sea ice meltwater on the alkalinity of seawater. *J. Mar. Res.* **41**, 43–52.

Jones, E. M., Bakker, D. C. E., Venables, H. J., Whitehouse, M. J., Korb, R. E., and co-authors. 2010. Rapid changes in surface water carbonate chemistry during Antarctic sea ice melt. *Tellus B*. **62B**, 621–635.

Jones, E. P. and Coote, A. R. 1981. Oceanic CO$_2$ produced by the precipitation of CaCO$_3$ from brines in sea ice. *J. Geophys. Res.* **86**, 11 041–11 043.

Jutterström, S. and Anderson, L. G. 2010. Uptake of CO$_2$ by the Arctic Ocean in a changing climate. *Mar. Chem.* **122**, 96–104.

Kelley, J. 1967. Carbon dioxide in seawater under the arctic ice. *Nature* **218**, 862–864.

Killawee, J. A., Fairchild, I. J., Tison, J.-L., Janssens, L. and Lorrain, R. 1998. Segregation of solutes and gasses in experimental freezing of dilute solutions: implications for natural glacial systems. *Geochim. Cosmochim. Acta* **62**, 3637–3655.

Kwok, R., Cunningham, G. F., Wensnahan, M., Rigor, I., Zwally, H. J., and co-authors. 2009. Thinning and volume loss of the Arctic Ocean sea ice cover: 2003–2008. *J. Geophys. Res.* **114**, C07005, doi:10.1029/2009JC005312.

Loose, B., Schlosser, P., Perovich, D., Ringelberg, D., Ho, D. T. and co-authors. 2011. Gas diffusion through columnar laboratory sea ice: implications for mixed-layer ventilation of CO2 in the seasonal ice zone. *Tellus* **63B**, 23–39.

Martinson, D. G. and Steele, M. 2001. Future of the Arctic sea ice cover: implications of an Antarctic analog. *Geophys. Res. Lettt.* **28**(2), 307–310.

McLaren, A. J., Banks, H. T., Durman, C. F., Gregory, J. M., Johns, T. C. and co-authors. 2006. Evaluation of the sea ice simulation in a new coupled atmospheric-ocean climate model (HadGEM1). *J. Geophys. Res.* **111**, C12014, doi:10.1029/2005JC003033.

Mikkelsen, D. M., Rysgaard, S. and Glud, R. N. 2008. Microalgal composition and primary production in Arctic sea ice: a seasonal study from Kobbefjord (Kangerluarsunnguaq), West Greenland. *Mar. Ecol. Prog. Ser.* **368**, 65–74, doi:10.3354/meps07627.

Mucci, A., Lansard, B., Miller, L. A. and Papakyriakou, T. N. 2010. CO$_2$ fluxes across the air-sea interface in the southeastern Beaufort Sea: ice-free period. *J. Geophys. Res.* **115**, C04003, doi:10.1029/2009JC005330.

Nedashkovsky, A. P., Khvedynich, S. V. and Petovsky, T. V. 2009. Alkalinity of sea ice in the high-latitudinal arctic according to the surveys performed at north pole drifting station 34 and characterization of the role of the arctic in the CO$_2$ exchange. *Mar. Chem.* **49**, 55–63, doi:10.1134/s000143700901007x.

Nomura, D., Yoshikawa-Inoue, H. and Toyota, T. 2006. The effect of sea-ice growth on air-sea CO$_2$ flux in a tank experiment. *Tellus* **58B**, 418–426, doi:10.1111/j.1600-0889.2006.00204.x.

Notz, D. and Worster, M. G. 2009. Desalination processes of sea ice revisited. *J. Geophys. Res.* **114**, C05006, doi:10.1029/2008JC004885.

Omar, A., Johannessen, T., Bellerby, R. G. J., Olsen, A., Anderson, L. G., and co-authors. 2005. Sea-ice and brine formation in Storfjorden: implications for Arctic wintertime air-sea CO$_2$ flux. In: *The Nordic Seas: An Integrated Perspective* (eds Drange, H., Dokken, T., Furevik, T., Gerdes, R. and Berger W.) Geophysical Monograph 158, American Geophysical Union, Washington, DC, 117–187.

Papadimitriou, S., Kennedy, H., Kattner, G., Dieckmann, G. S. and Thomas, D. N. 2003. Experimental evidence for carbonate precipitation and CO$_2$ degassing during sea ice formation. *Geochim. Cosmochim. Acta* **68**, 1749–1761, doi:10.1016/j.gca.2003.07.004.

Petrich, C. and Eicken, H. 2010. Growth, structure and properties of sea ice. In: *Sea Ice*. 2nd Edition. (ed. Thomas, D. N. and Dieckmann, G. S.). Wiley-Blackwell, Oxford, UK, 23–78.

Rudels, B., Björk, G., Nilsson, J., Winsor, P., Lake, I. and co-authors. 2005. The interaction between waters from the Arctic Ocean and the Nordic Seas north of Fram Strait and along the East Greenland Current: results from the Arctic Ocean-02 Oden expedition. *J. Marine Syst.* **55**, 1–30, doi:10-1016/j.jmarsys2004.06.008.

Rysgaard, S., Bendtsen, J., Pedersen, L. T., Ramløv, H. and Glud, R. N. 2009. Increased CO$_2$ uptake due to sea ice growth and decay in the Nordic Seas. *J. Geophys. Res.* **114**, C09011, doi:10.1029/2008JC005088.

Rysgaard, S., Glud, R. N., Sejr, M. K., Bendtsen, J. and Christensen, P. B. 2007. Inorganic carbon transport during sea ice growth and decay: a carbon pump in polar seas. *J. Geophys. Res.* **112**, C03016, doi:10.1029/2006JC003572.

Rysgaard, S., Nielsen, T. G. and Hansen, B. W. 1999. Seasonal variation in nutrients, pelagic primary production and grazing in a high-Arctic coastal marine ecosystem, Young Sound, Northeast Greenland. *Mar. Ecol. Prog. Ser.* **179**, 13–25.

Rysgaard, S., Thamdrup, B., Risgaard-Petersen, N., Fossing, H., Berg, P. and co-authors. 1998. Seasonal carbon and nutrient mineralization in a high-Arctic coastal marine sediment, Young Sound, Northeast Greenland. *Mar. Ecol. Prog. Ser.* **175**, 261–276.

Sabine, C. L., Feely, R. A., Gruber, N., Key, R. M., Lee, K. and co-authors. 2004. The oceanic sink for anthropogenic CO_2. *Science* **305**, 367–371.

Sejr, M. K., Krause-Jensen, D., Rysgaard, S., Sørensen, L. L., Christensen, P. B., and co-authors. 2011. Air-sea flux of CO_2 in arctic coastal waters influenced by glacier melt water and sea ice. *Tellus B*, doi:10.1111/j.1600.0889.2011.00540.x

Semiletov, I., Makshtas, A., Akasofu, S.-I. and Andreas, E. L. 2004. Atmospheric CO_2 balance: the role of Arctic sea ice. *Geophys. Res. Lett.* **31**, L05121, doi:10.1029/2003GL017996.

Shcherbina, A. Y., Talley, L. D. and Rudnick, D. L. 2003. Direct observations of North Pacific ventilation: Brine rejection in the Okhotsk Sea. *Science* **302**, 1952–1955.

Skogseth, R., Haugan, P. M. and Haarpaintner, J. 2004. Ice and brine production in Storfjorden from four winters of satellite and in situ observations and modeling. *J. Geophys. Res.*, **109**, C10008, doi:10.1029/2004JC002384.

Takahashi, T., Sutherland S. C., Wanninkhof, R., Sweeney, C., Feely, R. A., and co-authors. 2009. Climatological mean and decadal changes in surface ocean pCO$_2$, and net sea-air CO_2 flux over the global oceans. *Deep-Sea Res. II* **56**, 554–577.

Tison, J.-L., Haas, C., Gowing, M. M., Sleewaegen, S. and Bernard, A. 2002. Tank study of physio-chemical controls on gas content and composition during growth of young sea ice. *J. Glaciol.* **48**, 177–191.

Weeks, W. F. and Ackley, S. F. 1986. The growth, structure and properties of sea ice. In: *The Geophysics of Sea Ice* (ed. Untersteiner, N.). Plenum, New York.

Worby, A. P., Geiger, C. A., Paget, M. J., van Woert, M. L., Ackley, S. F., and co-authors. 2008. Thickness distribution of Antarctic sea ice. *J. Geophys. Res.* **113**, C05S92, doi:10.1029/2007JC004254.

Yamamoto-Kawai, M., McLaughlin, F. A., Carmack, E. C., Nishino, S. and Shimada, K. 2009. Aragonite undersaturation in the Arctic Ocean: effects of ocean acidification and sea ice melt. *Science* **326**, 1098–1100.

Zeebe, R. E. and Wolf-Gladrow, D. A. 2001. *CO$_2$ in Seawater: Equilibrium, Kinetics, Isotopes (Oceanography Series)*. Volume 65, Elsevier, Amsterdam, 346.

Zhang, J. 2007. Increasing Antarctic sea ice under warming atmospheric and oceanic conditions. *J. Clim.* **20**, 2515–2529.